Molecular characterization of gustatory second-order neurons reveals integrative mechanisms of gustatory and metabolic information

Rubén Mollá-Albaladejo[1], Manuel Jiménez-Caballero[1] and Juan A. Sánchez-Alcañiz[1]*

[1]Instituto de Neurociencias, CSIC-UMH, San Juan de Alicante, Spain
*Corresponding author
email: juan.sanchez@umh.es

Abstract

Animals must balance the urgent need to find food during starvation with the critical necessity to avoid toxic substances to ensure their survival. In *Drosophila*, specialized Gustatory Receptors (GRs) expressed in Gustatory Receptor Neurons (GRNs) are critical for distinguishing between nutritious and potentially toxic food. GRNs project their axons from taste organs to the Subesophageal Zone (SEZ) in the Central Brain (CB) of *Drosophila*, where gustatory information is processed. Although the roles of GRs and GRNs are well-documented, the processing of gustatory information in the SEZ remains unclear. To better understand gustatory sensory processing and feeding decision-making, we molecularly characterized the first layer of gustatory interneurons, referred to as Gustatory Second Order Neurons (G2Ns), which receive direct input from GRNs. Using trans-synaptic tracing with *trans*-Tango, cell sorting, and bulk RNAseq under fed and starved conditions, we discovered that G2Ns vary based on gustatory input and that their molecular profile changes with the fly's metabolic state. Further data analysis has revealed that a pair of neurons in the SEZ, expressing the neuropeptide Leucokinin (SELK neurons), receive simultaneous input from GRNs sensing bitter (potentially toxic) and sweet (nutritious) information. Additionally, these neurons also receive inputs regarding the starvation levels of the fly. These results highlight a novel mechanism of feeding regulation and metabolic integration.

Introduction

Animals face constant dangers in their environment that they must avoid to survive, being starvation and poisoning two critical threats. To prevent death by starvation, animals must continually seek food, even if it means risking consumption of potentially harmful substances[1-3]. Therefore, accepting or rejecting food containing potentially poisonous compounds will depend on the general nutritious content and toxicity of the meal, together with the starvation level of the animal. Similar to other animals, *Drosophila melanogaster* can discern different

taste qualities (sweet, bitter, salty, sour, umami or carbonation) through various populations of Gustatory Receptor Neurons (GRNs) tuned to each of these qualities[4]. GRNs are distributed across the *Drosophila*'s body including the proboscis, legs, wing margins, and the ovipositor organ, expressing a combination of receptors for detecting various food compounds[5]. There are four major families of receptors involved in gustatory perception: Gustatory Receptors (GRs), Ionotropic Receptors (IRs), Transient Receptor Proteins (TRPs), and pickpocket (ppk) channels[6]. Specific GRNs are associated with particular valences, such as sweet or bitter tastes. For instance, Gr64f is a receptor for sugar detection promoting feeding behavior[7,8], while Gr66a is present in GRNs that detect bitter compounds leading to feeding rejection[9,10].

GRNs project their axons to the Subesophageal Zone (SEZ), the main brain region in flies for integrating and processing gustatory information. Unlike the olfactory system, where olfactory sensory neurons expressing the same receptors converge in the same glomeruli to synapse with projection neurons, the gustatory system lacks such anatomical subdivisions[5,11]. However, neurons expressing receptors that respond to sweet compounds and elicit attractive behaviors converge in specific SEZ regions without overlapping neurons detecting bitter compounds and inducing feeding rejection[1,2].

The development of extensive collections of Gal4 lines[12], split-Gal4 collections[13], and databases for searchable neurons[14], has facilitated the identification of gustatory interneurons in the SEZ involved in feeding behavior. Those databases have been used to design experimental procedures that has help to the identification of some gustatory interneurons involved in integrating gustatory information and inducing feeding[1,15–21]. These studies have identified command neurons critical for feeding behavior, some directly receiving input from GRNs, such as certain GABAergic neurons[22], while others, like the Feeding neuron (Fdg), act as a hub to control food acceptance without being connected directly to any GRN[1]. Despite these advances, the role of gustatory interneurons in integrating gustatory information and the metabolic state of the fly remains largely unexplored. The recent development of the *Drosophila* brain connectome through electron microscopy is advancing our understanding of SEZ connectivity and the complex interactions among GRNs[2,3].

We have aimed to elucidate the integration of gustatory information and the metabolic state, by analyzing the first layer of interneurons that collect gustatory information, Gustatory Second-Order Neurons (G2Ns[23]). We have decided to focus on understanding how flies integrate gustatory information that codes for opposing behaviors: sweet tastants elicit feeding whereas bitter compounds induce food rejection[11]. We have followed a molecular approach to identify G2Ns. First, we employed the *trans*-Tango genetic tool[24], which labels postsynaptic neurons connected to specific presynaptic neurons. Later, using Fluorescent Activated Cell Sorting (FACS) of labeled G2Ns and bulk RNA sequencing (RNAseq), we characterized the molecular profiles of postsynaptic neurons connected to sweet and bitter GRNs in fed and

starved conditions for the first time. These analyses show that G2Ns receive input from molecularly distinct GRNs, and their transcriptional profiles change upon starvation, presumably to adapt to the new metabolic state. Using connectomic techniques, we further demonstrate that the two Leucokinin-expressing neurons in the SEZ (SELK neurons) are G2Ns that simultaneously receive sweet and bitter GRN input. Behavioral experiments revealed that these two neurons integrate information regarding the metabolic state of the fly and are involved in the processing of bitter and sweet information that impacts the initiation of feeding behavior.

Results

Molecular characterization of gustatory second-order neurons

We employed the recently described trans-synaptic tracing method, *trans*-Tango[24], to label G2Ns synaptically connected to sweet and bitter GRNs. To label G2Ns receiving sweet information, we used the *Gr64f-Gal4* transgene[7,10], and for G2Ns receiving bitter information, we used the *Gr66a-Gal4* transgene [10,25]. These Gal4 transgenes enabled us to label multiple G2Ns of interest (**Supplementary Figure 1.1A and B**). The number of postsynaptic G2Ns differed between the GRNs, indicating differences in information processing for different tastants (**Supplementary Figure 1.1C and D**). Since satiety and hunger significantly influence behavior, modifying olfactory behavior[26], memory formation[27] and food consumption[2,28], we extended our analysis to characterize molecularly G2Ns receiving different gustatory inputs in two metabolic states: fed and 24-hour starved flies. Since all G2Ns are fluorescently labeled with mtdTomato, we used FACS to separate and collect the cells for sweet and bitter G2N populations ($Gr64f^{G2N}$ and $Gr66a^{G2N}$, respectively) in the two metabolic conditions (fed and starved) (See Materials and Methods for a detailed description of the sorting procedure and sample number in **Table 1**). We then performed bulk RNAseq for each condition (**Figure 1A**).

The data's Principal Component Analysis revealed that the transcriptomic profiles of the two G2N populations are different and that the metabolic state (fed vs. starved) significantly influences gene expression without affecting the separation among the populations in the PC space (**Figure 1B**). These findings suggest that the first layer of neurons collecting sensory information is already modulated by the fly's metabolic state, potentially impacting subsequent information processing.

We further analyzed the changes in gene expression between fed and starved conditions across the two G2N populations. Many genes exhibited differential expression in starved flies compared to fed flies (**Figure 1C**). Gene Ontology (GO) analysis indicated that several genes were involved in nervous system development and synapse organization,

suggesting the importance of synapse remodeling during starvation adaptation. Additionally, GO terms related to the response to sensory stimuli and stress response were identified, implying that starvation induces molecular signatures of stress in flies. Finally, some genes associated with signaling pathways indicated that neurotransmitter and neuropeptide signaling processes might be altered during starvation, leading to specific adaptations in the neuronal circuits involving G2Ns (**Supplementary Figure 1.2**).

Characterization of neurotransmitter and neuropeptide expression

Next, we focused on the expression of neurotransmitters, neuropeptides, and their respective receptors, as they are known to modulate feeding, among many other behaviors[29]. For example, the CCHamide 1 receptor regulates starvation-induced olfactory modulation[30], NPF (Neuropeptide F) modulates taste perception in starved flies by increasing sensitivity to sugar and decreasing sensitivity to bitter by promoting GABAergic inhibition onto bitter GRNs[2]; starvation enhances behavioral sugar-sensitivity via increased dopamine release onto sweet GRNs, indirectly decreasing sensitivity to bitter tastants[31]; and octopamine signaling affects bitter signaling in starved flies[3].

Our RNAseq data revealed that the most prominent neurotransmitter receptor expressed in all G2Ns was *nAChRbeta1* (nicotinic Acetylcholine Receptor Beta 1) (**Figure 2A**). This is consistent with previous findings showing that GRNs are mostly cholinergic[32]. Other acetylcholine receptors were also expressed in G2Ns and receptors for other neurotransmitters. This indicates that while G2Ns receive significant input from GRNs, they also integrate information from a complex network of other neurons using different neurotransmitters. We found no variation in expression levels for any neurotransmitter receptors when comparing fed and starved conditions. Regarding neurotransmitter expression, *Gad1* (Glutamic acid decarboxylase 1) and *Ddc* (Dopa decarboxylase), two essential enzymes involved in the synthesis of GABA and dopamine, respectively, were highly expressed in the two G2N populations, and both metabolic states (**Figure 2B**). Other enzymes involved in the GABA pathway, like *VGAT* (vesicular GABA transporter) or *GABAT* (γ-aminobutyric acid transaminase), were also expressed but at lower levels than *Gad1*. Similarly, other enzymes or transporters related to other neurotransmitters, like glutamate (Glu) or serotonin (5-HT), were present but at lower levels.

Regarding neuropeptide receptors, we found many receptors expressed in all G2N populations with varying expression levels (**Figure 2C**). For instance, the *EcR* (Ecdyson Receptor) showed expression in all three populations with a slight decrease under starvation, indicating a possible role in adapting to food deprivation. Additionally, *sNPF-R* was highly

expressed with similar expression patterns as its ligand sNPF, highlighting the importance of sNPF and its signaling pathway in regulating starvation and feeding[33–35].

Neuropeptides showed variable expression patterns between populations and conditions (**Figure 2D**). For example, *sNPF* was highly expressed in all G2Ns, particularly in the Gr66a^{G2N} population, without changes associated with the metabolic state. sNPF (short Neuropeptide F) production, which is related to circulating sucrose levels, impacts food intake by integrating sweet and bitter information in food-deprived flies[2]. This highlights the role of sNPF and its receptor (sNPF-R) in regulating the feeding behavior according to the metabolic state, as it is secreted in the midgut and by neurosecretory cells in the brain. Dh31 (diuretic hormone 31) and Dh44 (Diuretic hormone 44) both involved in desiccation tolerance and starvation adaptation[36], also showed notable expression in both G2N populations under both starved and fed conditions. Nplp1 (Neuropeptide-like precursor 1), which is associated with synaptic organization in the nervous system and water balance[29], was also expressed in both G2Ns. Among all neuropeptides, however, Leucokinin (Lk) displayed the most striking expression change among all neuropeptides. Though Lk has no (or very low) expression in the Gr64f^{G2N} population under fed and starved conditions and no (or very low) expression in the Gr66a^{G2N} under fed conditions, Lk showed significantly elevated expression in the Gr66a^{G2N} population under starved conditions. This expression pattern specific to Gr66a^{G2Ns} suggests that Lk may play a role in processing bitter information under starvation. We decided to explore this neuropeptide further to understand its role in integrating feeding behavior and the metabolic state of the flies.

Leucokinin expression is upregulated in SELK neurons in the starved condition

Leucokinin (Lk) is a neuropeptide with multiple roles in various physiological and behavioral processes[37]. Three different Lk neuron groups exist in the adult *Drosophila* Central Nervous System (CNS). There are approximately 20 Lk neurons in the Ventral Nerve Cord (ABLKs), while in the CB, there are four Lk neurons, two located in the Lateral Horn (LHLK) and another two located in the SEZ (SELK)[38,39]. ABLKs use Lk as a hormonal signal targeting peripheral tissues, including renal tubules, to regulate water and ion homeostasis in response to desiccation, starvation, and ion stress, as Lk regulates fluid secretion in the Malpighian (renal) tubules[39]. LHLK neurons are part of the output circuitry of the circadian clock, regulating locomotor activity and sleep suppression induced by starvation[40–43]. Functional imaging revealed that LHLK neurons, not SELK neurons, were required to suppress sleeping during starvation[43]. It has been suggested that SELK neurons may regulate feeding as possible synaptic partners to the premotor feeding program. However, it is still not clear the role of SELK neurons in feeding behavior[37,39].

Due to the dissection method used for our RNAseq experiment, we primarily captured SELK neurons rather than LHLK neurons (**Figure 1A**). To confirm that starvation induces changes in Lk gene expression, we performed qPCR on brains from fed and starved *Drosophila*. Given that Lk neurons constitute 4 out of approximately 200.000 neurons in the *Drosophila* brain[44], we enriched our samples by expressing GFP in Lk neurons using the driver *Lk-Gal4*[45] combined with *UAS-mCD8:GFP* transgene and FACS sorting of the GFP^+ cells. We conducted qPCR analysis on the whole CB (including both LHLK and SELK neurons) as well as on the SEZ alone (containing only the 2 SELK neurons) in fed and starved conditions (**Figure 3A and 3B**). Our results showed that starvation increased the expression level of Lk mRNA in the CB and also in the SELK neurons, indicating that Lk expression is indeed affected by the animal's starvation state (**Figure 3C**). To confirm that the increased mRNA expression translates into higher protein levels, we performed immunohistochemistry using an Lk antibody in fed and 24-hour starved wild-type flies. We quantified the fluorescence in the LHLK and SELK neurons and found that Lk expression was elevated under starvation conditions (**Figure 3D-F**) further validating our RNAseq results. Together, these three lines of evidence indicate that SELK neurons increase the expression of the Lk neuropeptide in 24-hour starved flies.

<u>*Leucokinin neurons are gustatory second order neurons to GRNs*</u>

Our RNAseq data showed that the two SELK neurons receive almost exclusive input from bitter but not sweet GRNs and that the metabolic state of the fly modulates the expression of Lk. To confirm that Lk neurons are indeed postsynaptic partners of bitter GRNs, we used an Lk antibody[38] to test the co-localization of Lk protein with the cells labeled in *GRNs-Gal4>trans-Tango* flies. These experiments demonstrated that Lk signal colocalizes with trans-Tango in *Gr66a-Gal4>trans-Tango* flies, confirming our expectations based on the RNAseq data (**Figure 4A**). Unexpectedly, however, we also found colocalization of the Lk antibody signal in *Gr64f-Gal4>trans-Tango* flies, suggesting that SELK neurons do not receive exclusive input from bitter neurons but also from sweet-sensing neurons expressing the Gr64f receptor (**Figure 4B**).

To validate the synaptic connectivity between $Gr64f^{GRNs}$ and $Gr66a^{GRNs}$ with SELK neurons, we next used the GRASP (GFP Reconstruction Across Synaptic Partners)[46] technique. GRASP can reveal the synaptic connectivity between two neurons through the expression of half of the GFP protein in each candidate neuron. The reconstruction of the entire GFP protein in the synaptic cleft can be detected by a specific GFP antibody. We expressed half of the GFP (GFP^{11}) protein in the bitter GRNs using *Gr66a-LexA*[47] and sweet GRNs using *Gr64f-LexA*[8] transgenes. The other half of GFP (GFP^{1-10}) protein was expressed

in Lk neurons using the *Lk-Gal4* driver. GRASP results confirmed the synaptic connection between bitter GRNs and sweet GRN with SELK neurons in the SEZ (**Figure 5A**), further confirming our *trans*-TANGO previous result. Additionally, we used BacTrace[48] to confirm that the connectivity between Gr64f^{GRNs} and Gr66a^{GRNs} neurons with SELK neurons is real. This technique works similarly to *trans*-Tango, but while *trans*-Tango labels all postsynaptic neurons, BacTrace labels presynaptic partners. For our experiments, we used *Gr66a-LexA* and *Gr64f-LexA* as candidate presynaptic partners. Consistent with the GRASP results, our BacTrace experiment indicated that sweet and bitter GRNs are presynaptic to SELK neurons (**Figure 5B**), further supporting a model in which Lk neurons are G2Ns receiving input from Gr64f^{GRNs} and Gr66a^{GRNs}. To our best knowledge, this is the first time a G2N has been identified as collecting information from two populations of GRNs that transduce sensory information of different valence, sweet-attractive, and bitter-repulsive.

Connectivity of SELK neurons within the Drosophila brain

Using orthogonal molecular techniques, we have demonstrated that the expression of Lk neuropeptide upregulates its expression in SELK neurons during starvation and that they are G2Ns to both sweet Gr64f^{GRNs} and bitter Gr66a^{GRNs}. To more broadly characterize SELK neurons and their connectivity, we employed the connectome from a Full Adult Female Brain (FAFB) EM volume[49]. Recently, Engert et al., 2022[50], used the FAFB to identify groups of bitter and sweet-sensing GRNs, their projections to the SEZ, synaptic contacts among the GRNs (including those expressing Gr64f and Gr66a), and their possible synaptic partners. We reasoned that because the SELK neurons receive input from bitter and sweet GRNs, we could identify the SELK neurons in the FAFB as receiving input from the identified Gr64f^{GRNs} and Gr66a^{GRNs}. Using the dataset from Engert et al., we identified all postsynaptic partners to the Gr64f^{GRNs} and Gr66a^{GRNs} described without limiting the number of synaptic contacts among neurons to consider them as synaptic partners (See materials and methods for a detailed description).

We identified a total of 12594 postsynaptic hits to the Gr66a^{GRNs,} and a total of 36790 hits for the Gr64f^{GRNs} analyzed. We intersected both datasets and obtained a total of 351 downstream segment IDs as possible G2Ns receiving Gr64f^{GRN} and Gr66a^{GRN} input. After visual morphological comparison between the SELK neuron candidates and the SELK arborization (**Figure 3A**), we concluded that only one neuron with ID segment 720575940623529610 (or 720575940632524559 ID as both labels the same neuron)) was a strong candidate to be the Left SELK neuron (**Figure 6A, magenta**). Using the FlyWire Codex tool, we identified this neuron as GNG.276 (Gnathal Neuron Ganglia 276), a type DNg70 neuron putative GABAergic, based on previous annotation and proofreading by the FlyWire

community[51,52]. Using the NBLAST online morphology tool from FlyWire, we searched for neurons with similar arborizations to GNG.276 and found GNG.246 (ID: 720575940632407826) as the Right SELK neuron (**Figure 6A, cyan**).

To further analyze the connectivity of these neurons, we looked for the pre-and postsynaptic organization of SELK neurons. We only considered those synaptic partners with ≥10 synaptic connections to limit possible false positive synaptic connections. Most of the postsynaptic partners of SELK neurons (184) localized in the SEZ, as revealed by the BrainCircuit analysis[53] (**Figure 6B**), with significant projections to the pars intercerebralis. This region contains Insulin Producing Cells (IPCs) neurons that project to the tritocerebrum in the SEZ, where a significant concentration of fibers can be appreciated in the *trans*-Tango immunohistochemistry (**Figure 6C**). This data supports previous results showing that IPC neurons express the Lk receptor (Lkr) and that they may be modulated by Lk-expressing neurons[39,43]. We found only one bitter (GRN R2#5) and one sweet (GRN R4#17) GRN as presynaptic candidates to GNG.276 (right SELK neuron), and only one sweet GRN (R4#14) presynaptic to GNG.246 Lleft SELK neuron). That so few presynaptic GRNs were found indicates that SELK proofreading is still required for a much more precise assembly and annotation of the FAFB dataset. We identified a total of 84 presynaptic partners using BrainCircuits with a complex distribution over the brain (**Figure 6D**), though most of the connectivity was found within the SEZ. Additionally, we used *retro*-Tango[54], a retrograde trans-synaptic technique that employs similar trans-synaptic mechanisms as *trans*-Tango but in the retrograde direction. This experiment showed that SELK neurons receive most of the presynaptic input from neurons located in the SEZ (**Figure 6E**), consistent with the data derived from the FAFB analysis. Encouragingly, we observed a significant concentration of synapsis at the tritocerebrum, similar to the *trans*-Tango signal. Those results might suggest that SELK neurons also send information to the IPC neurons.

Leucokinin modulates feeding behavior

We have shown that Lk neurons receive direct input from bitter and sweet GRNs and that the expression of the neuropeptide Lk is sensitive to the starvation level of the animal. Considering that Gr64f^{GRNs} collect sweet information that initiates feeding, while Gr66a^{GRNs} transduce bitter information that inhibits feeding, we wondered how Lk neurons modulate feeding by integrating gustatory and metabolic information. It has been previously shown that silencing Lk neurons affected the ability of the flies to respond to sucrose in a Proboscis Extension Response (PER) experiment[39]. We decided to silence all Lk neurons of *Drosophila* using the *Lk-Gal4* driver expressing the tetanus toxin (TNT) using the *UAS-TNT* transgene and *UAS-TNT^{imp}* transgene as control[55] and test the response of these flies in PER assay (**Figure 7A,**

Experiment 1). In our hands, silencing Lk neurons had no effect on the ability of the flies to respond to increasing concentrations of sucrose in our PER assay in 24-hour starved flies (**Figure 7B**). The differences between both studies might be due to differences in the handling and stimulus methodology[39].

Since Lk neurons receive input from Gr64f^{GRNs} and Gr66a^{GRNs}, we reasoned they might be involved in integrating sweet and bitter information. We decided to test whether LK neurons played any role in PER towards sweet food containing bitter compounds, as it has been shown PER to sucrose is affected by the presence of bitter substances[56]. For that purpose, we used a concentration of sucrose that would not saturate PER response (50mM Sucrose), and mixed it with increasing concentrations of caffeine, a bitter compound known to reduce PER response upon sucrose stimulation (**Figure 7A, Experiment 2**). The PER experiment was performed in fed, 12-hour and 24-hour starved flies (**Figure 7C**). As expected, fed flies showed a low response to PER for 50mM sucrose and the addition of caffeine reduced the response to sucrose similarly in control and experimental flies. Starved flies for 12 hours showed an increased response to sucrose compared to fed flies, and the addition of caffeine clearly reduced PER in a concentration-dependent manner. At high concentrations of caffeine, experimental flies showed a greater decrease in PER response. This result was more significant in flies starved for 24 hours. Increasing the concentration of caffeine decreased the PER response in control flies, but this decrease was larger in the experimental flies with Lk neurons silenced. These results suggest that Lk neurons are not essential for the response to sucrose alone but are needed for the proper integration of sucrose and caffeine, thus allowing feeding on bitter-laced food.

Because PER experiments only evaluate feeding initiation, we next wondered if Lk neurons were needed throughout feeding and employed the flyPAD[57] to monitor feeding behavior over a more extended period. In this setup, it is possible to offer two types of foods to individual flies and monitor their feeding patterns over at least 1 hour. Two experimental designs were implemented (**Figure 7D**). In experiment 1, we offered the flies the possibility to feed from food containing 20 mM sucrose and other food containing 100 mM sucrose. Typically, flies prefer the highest concentration of sucrose. If the highest concentration of sucrose is laced with a bitter compound (in our case, caffeine), the rejection of the highest concentration of sucrose and acceptance of the lowest concentration is directly related to the concentration of caffeine added. When flies with their Lk neurons silenced are placed in this two-choice assay, they showed a slight increase in preference to feed on the highest concentration of sucrose compared to the control flies (**Figure 7E**). However, adding caffeine did not affect the flies' ability to choose. In both cases, the number of sips each fly took was no different. While the PER experiments mainly test the role of SELK neurons, the 1-hour two-choice flyPAD assay involves silencing all Lk neurons (LHLK, SELK, and ABLK), suggesting that other

compensatory mechanisms might control the flies' ability to tolerate bitter-laced food. Our experiments show that SELK neurons are involved in initiating feeding on sweet food laced with bitter compounds, but their role in sustained feeding on such food remains elusive.

Discussion

We have demonstrated that Gustatory Second Order Neurons (G2Ns), which transduce opposing behaviors such as sweet attraction and bitter repulsion, exhibit molecular differences and undergo transcriptomic changes upon starvation. Molecular, connectomic, and behavioral experiments have identified SELK neurons as particularly dynamic G2Ns when under starved conditions. Surprisingly, we discovered that these neurons simultaneously collect information from sweet-sensing Gr64f^{GRNs} and bitter-sensing Gr66a^{GRNs}. Additionally, SELK neurons respond to starvation by increasing the neuropeptide Leucokinin (Lk) expression. Together, these findings reveal that SELK neurons play a novel role in modulating feeding initiation during starvation when flies are presented with sweet food laced with bitter compounds.

Our RNAseq data analysis revealed that SELK neurons only received input from Gr66a^{GRNs}. However, further analysis using immunohistochemistry (*GRN-Gal4>trans-Tango* + Lk immunohistochemistry) combined with GRASP and BacTrace, demonstrated that SELK neurons are G2Ns to Gr64f^{GRNs} and Gr66a^{GRNs}. To our knowledge, this is the first demonstration that a pair of G2Ns are broadly tuned to both bitter and sweet gustatory inputs while also integrating metabolic information (**Figure 8A**). *trans*-Tango and its variants have been successfully used to study connectivity and functionality in various neuronal circuits, including gustatory, olfactory, visual systems, mushroom body output neurons or clock neurons[24,58–61]. Recent analysis of the *retro*-TANGO tool, showed that a minimum number of synaptic connections between neurons is needed to label the postsynaptic neurons properly. It is possible that Gr64f^{GRNs} make less synaptic contacts with SELK neurons than Gr66a^{GRNs}, decreasing the probability of being labeled by *trans*-TANGO. Combined with our stringent FACS protocol, this could explain why we were unable to capture SELK neurons as Gr64f^{G2Ns} with FACS.

Current understanding suggests that tastant quality is mediated by labeled lines, where gustatory receptor neurons are segregated to respond to specific taste qualities[62]. This segregation is thought to persist further upstream in the circuit, as observed in mice, where taste cells respond to specific tastants and this information remains segregated at the geniculate ganglion[63], gustatory cortex[64], and the amygdala[65]. Similarly, in *Drosophila,* GRNs that detect bitter and sweet compounds project their axons to the SEZ in a non-overlapping fashion[10]. Whole-brain *in vivo* calcium imaging revealed that most SEZ interneurons respond to single tastants[66]. However, the same study identified neurons that may respond to multiple

tastants, like bitter and sweet, though specific neurons and their circuit positions were not detailed. Other SEZ neurons have been shown to integrate sweet and bitter inputs, such as the E49 motor neuron, which is stimulated by sweet input (Gr5a) and inhibited by bitter input (Gr66a)[67], but these are not G2Ns. We attempted *in vivo* calcium imaging to further study the gustatory integration in those neurons, but we were unsuccessful due to the challenging location of SELK somas in the medio-ventral region of the SEZ, which is obscured by the proboscis in many occasions even when fully extended. Additionally, variability in labeling using *UAS-GCaMP7s* and *UAS-GCaMP6m* lines hampered the proper imaging of these neurons. Our behavior experiments show that SELK neurons are early integrators of gustatory and metabolic information. However, our behavioral results point to the role of SELK neurons as an early hub that collects different types of information to drive feeding initiation.

In summary, our study highlights the complex integration of gustatory and metabolic information by SELK neurons, providing new insights into the neural mechanisms underlying feeding behavior in *Drosophila*. This work advances our understanding of how sensory and metabolic cues are integrated into the brain to regulate vital behaviors such as feeding.

Acknowledgments

We thank Prof. Richard Benton, Prof. Roman Arguello, and members of the JSA laboratory for their comments on the manuscript. We also thank our colleagues from the Institute of Neuroscience for their insightful inputs while developing the present research. This work was funded by the Spanish Research Agency, operating grants PID2019-105839GA-I00, CNS2022-135109 and Ramón y Cajal Fellowship RyC2019-026747-I.

Author contribution

JSA conceived the project and wrote the manuscript with RMA. JSA and RMA performed the brain dissections for the RNAseq analysis. RMA did the FACS sorting, RNA extraction, and sample preparation for sequencing. JSA performed the RNAseq analysis. RMA did the immunohistochemistry, connectomic analysis and PER behavior. MJC performed the flyPAD experiments.

Declaration of interests

The authors declare no competing interests.

Main text figures and figure legends

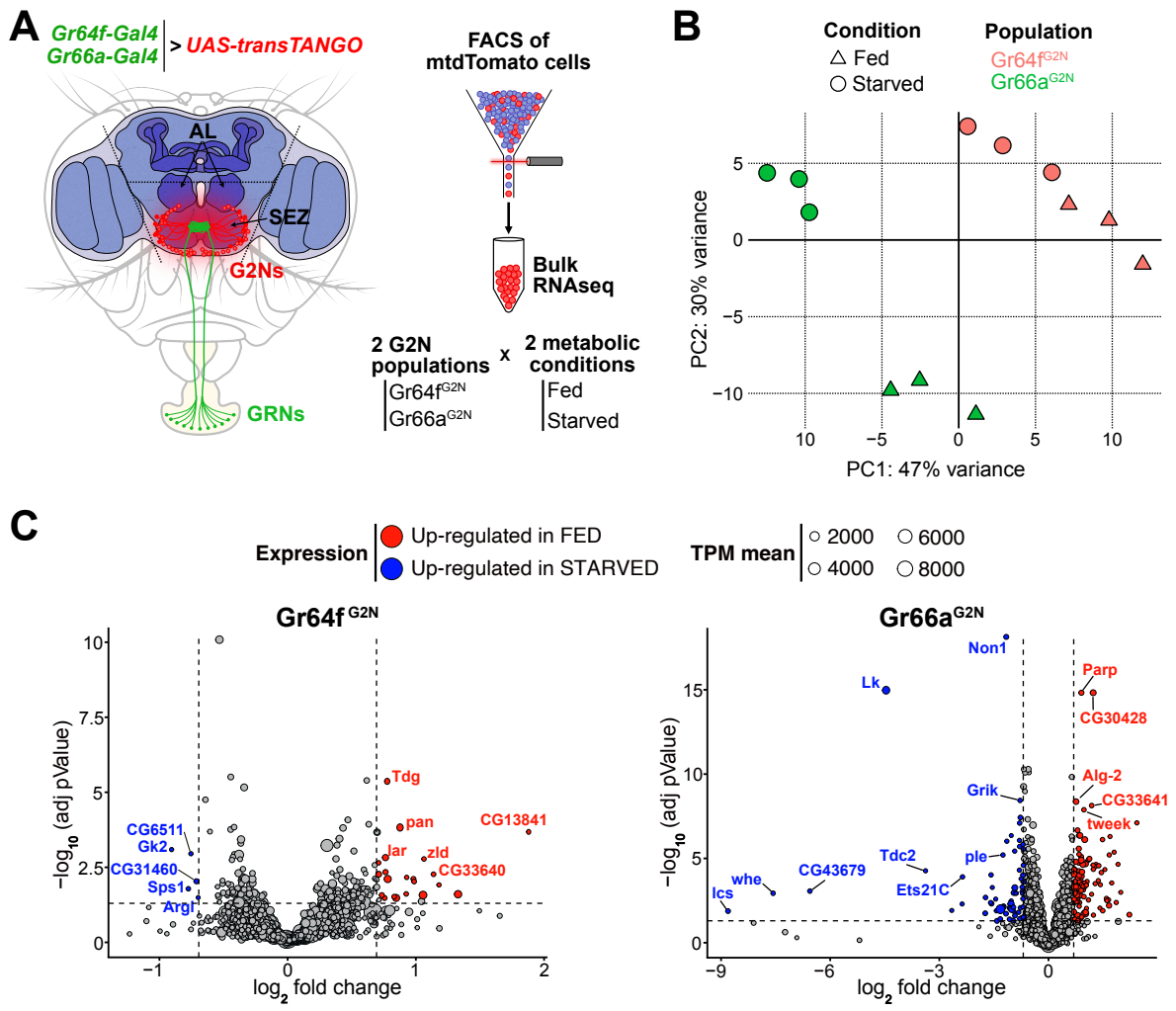

Figure 1. **The metabolic state affects the gene profiles of the Gustatory Second Order Neurons (G2Ns) populations analyzed**. (**A**) The scheme depicts the region of the brain dissected and the sorting of the G2Ns according to the input. Two populations of *trans-TANGO* neurons were labeled using *Gr64f-Gal4* and *Gr66a-Gal4* transgenic lines. Flies were either fed or food-starved for 24 hours. (**B**) Principal Component Analysis (PCA) of the genes. (**C**) Volcano plots show the genes up- and down-regulated in fed and starved conditions in the two populations of G2Ns.

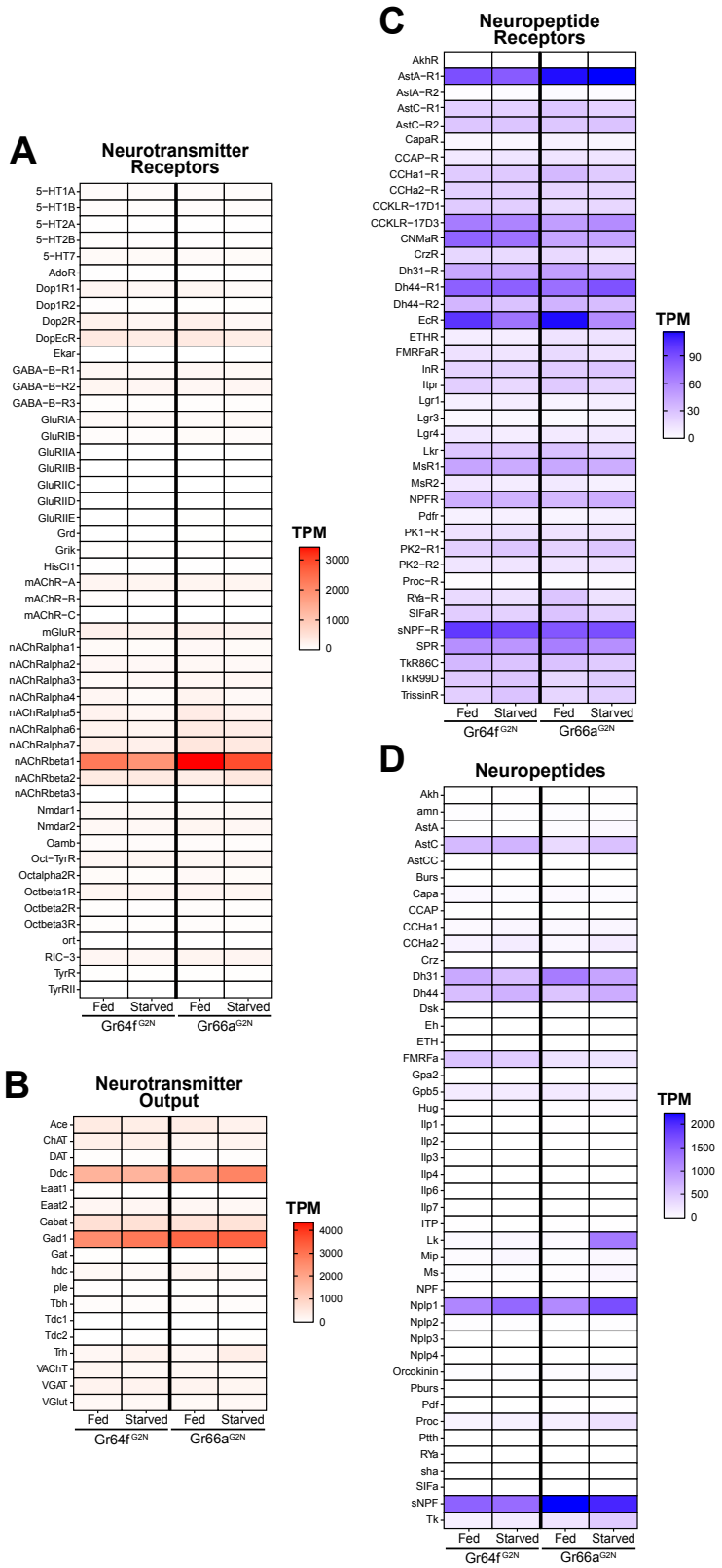

Figure 2. **Transcripts per Million (TPM) for Neuropeptides and Neurotransmitters**. TPMs for Neurotransmitters (**A**), Neurotransmitter Receptors (**B**), Neuropeptides (**C**) and Neuropeptide Receptors (**D**) for the two G2N populations in the two metabolic conditions studied (fed and 24h starved).

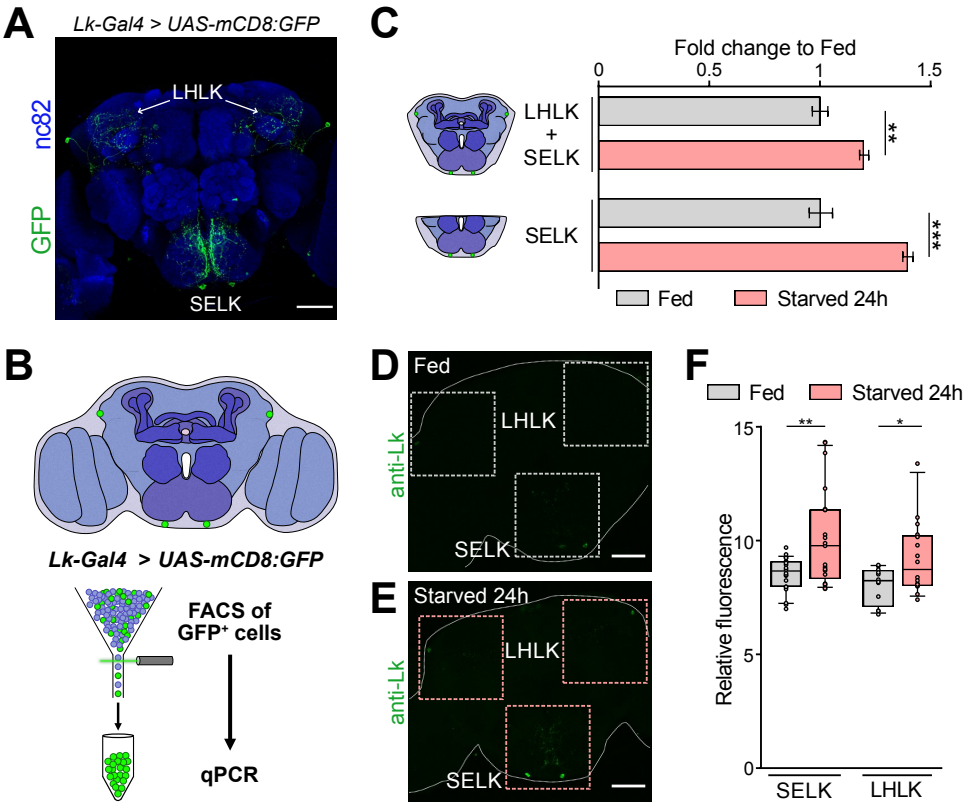

Figure 3. **Leucokinin expression is increased in starvation**. (**A**) Immunofluorescence with anti-GFP (green) and anti-nc82 (blue) on a whole-mount brain of a *lk-Gal4>UAS-mCD8:GFP*. (**B**) Scheme showing the approach used to select the Lk GFP$^+$ neurons by FACS. (**C**) qPCR results for Lk neurons labeled with GFP and sorted by FACS. The central brain includes all four Lk neurons, while the SEZ region includes only the two neurons located in this region. (**D**) Intensity fluorescence quantification in whole Oregon-R brains stained with anti-Lk antibody in fed and 24-hour starved flies. SELK Fed = 20 brains; SELK Starved = 21 brains; LHLK Fed = 12 brains; LHLK Starved = 16 brains. Scale bar = 50μm. Statistical test: Wilcoxon rank sum test. *p<0.05, **p<0,01, ****p < 0,0001. Scale bar = 50μm.

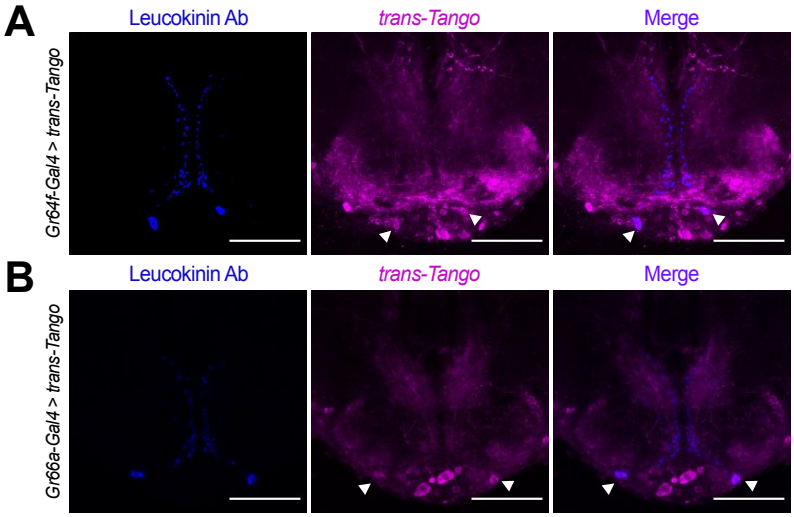

Figure 4. Lk neurons co-localize with the *trans*-Tango signal. Immunofluorescence with anti-Leucokinin (blue) and anti-RFP (magenta) on whole-mount brains of (**A**) *Gr64f-Gal4>trans-TANGO*, and (**B**) *Gr66a-Gal4>trans-TANGO*. Images correspond to the adult SEZ. Arrowheads point to SELK neurons. Scale bar = 50μm.

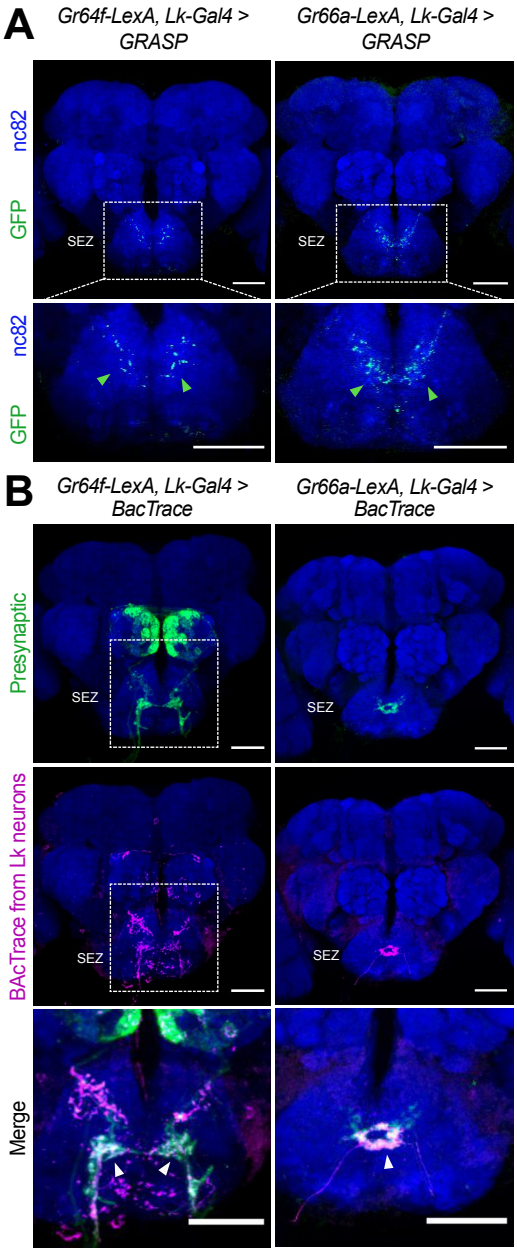

Figure 5. **Lk neurons are synaptically connected to Gr64f^{GRN} and Gr66a^{GRN}.** (**A**) Immunofluorescence with anti-GFP (green) and anti-nc82 (blue) on whole-mount brains of *Gr64f-LexA>LexAop-CD4spGFP^{11}* and *Lk-Gal4>UAS-CD4spGFP$^{1-10}$* (left column) and *Gr66a-LexA>LexAop-CD4spGFP^{11}* and *Lk-Gal4>UAS-CD4spGFP$^{1-10}$* (right column). Arrowheads point to GFP positive signal. (**B**) Immunofluorescence with anti-GFP (green), anti-RFP (magenta), and anti-nc82 (blue) on whole-mount brains of *Gr64f-LexA, Lk-Gal4>BacTrace* (left column) and *Gr66a-LexA, Lk-Gal4>BacTrace* (right column). Arrowheads point to the BacTrace positive signal. Scale bar = 50μm.

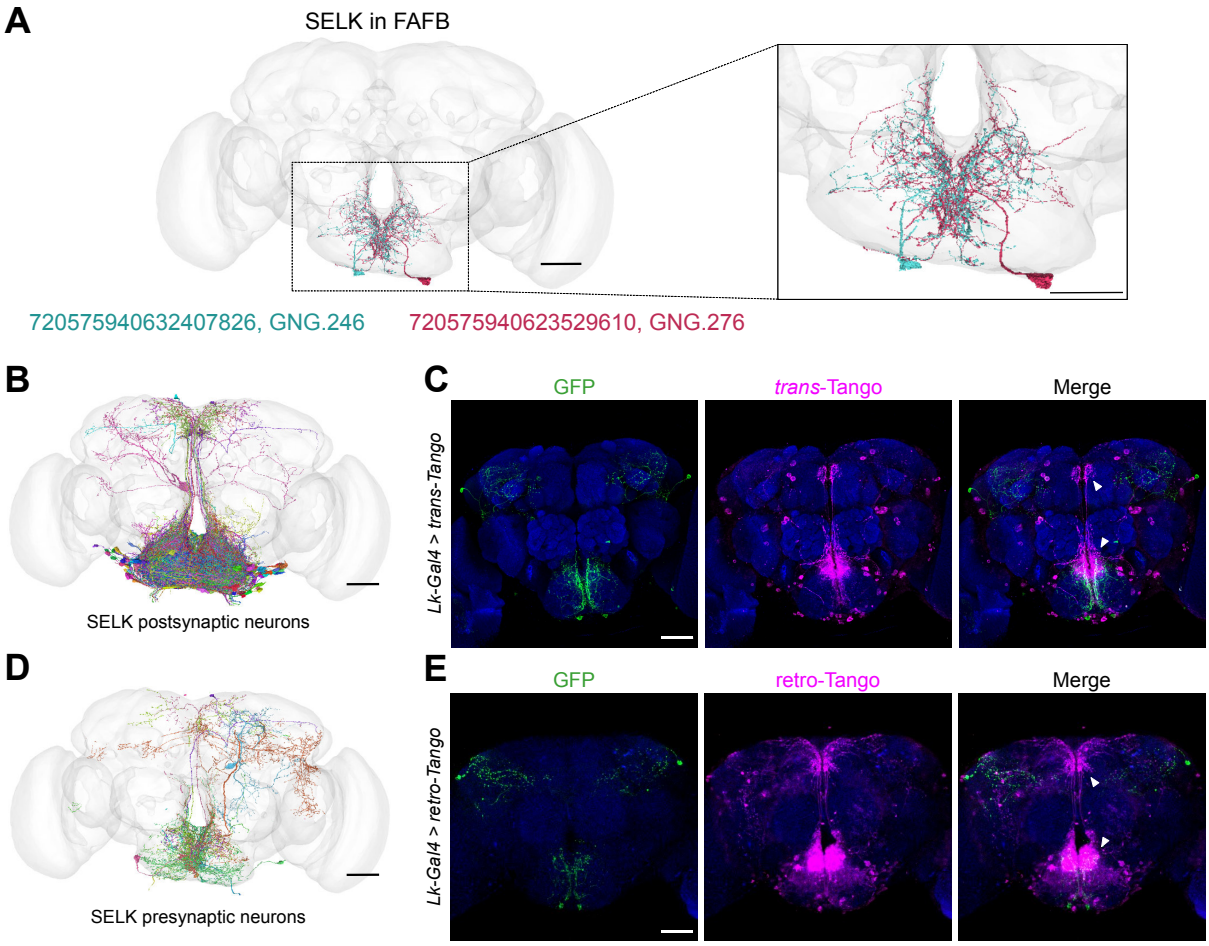

Figure 6. Lk neurons are pre- and postsynaptic to a significant number of neurons. (**A**) The anatomy of the SELK neurons (Right in cyan and Left in magenta) was reconstructed using the FAFB brainmesh template in Flywire. IDs from Flywire are indicated: 720575940632407826 ID for the Left SELK in cyan (GNG.246) and 720575940623529610 for the Right SELK in magenta (GNG.276). Zoom in to the SEZ from (A), showing the details of the neuronal arborizations. (**B**) SELK postsynaptic candidate neurons reconstructed in the FAFB brainmesh template in Flywire. Only postsynaptic candidate neurons with ≥10 synaptic points with SELK neurons are shown (174 postsynaptic candidate neurons). (**C**) Immunofluorescence with anti-GFP (green), anti-RFP (magenta), and anti-nc82 (blue) on a whole-mount brain on a *Lk-Gal4>trans-TANGO* flies. (**D**) SELK presynaptic candidate neurons reconstructed in the FAFB brainmesh template in Flywire. Only presynaptic candidate neurons with ≥10 synaptic points with SELK neurons are shown (84 presynaptic candidate neurons). (**E**) Immunofluorescence with anti-GFP (green), anti-RFP (magenta), and anti-nc82 (blue) on a whole-mount brain on a *Lk-Gal4>retro-TANGO* flies. Scale bars: 50 µm.

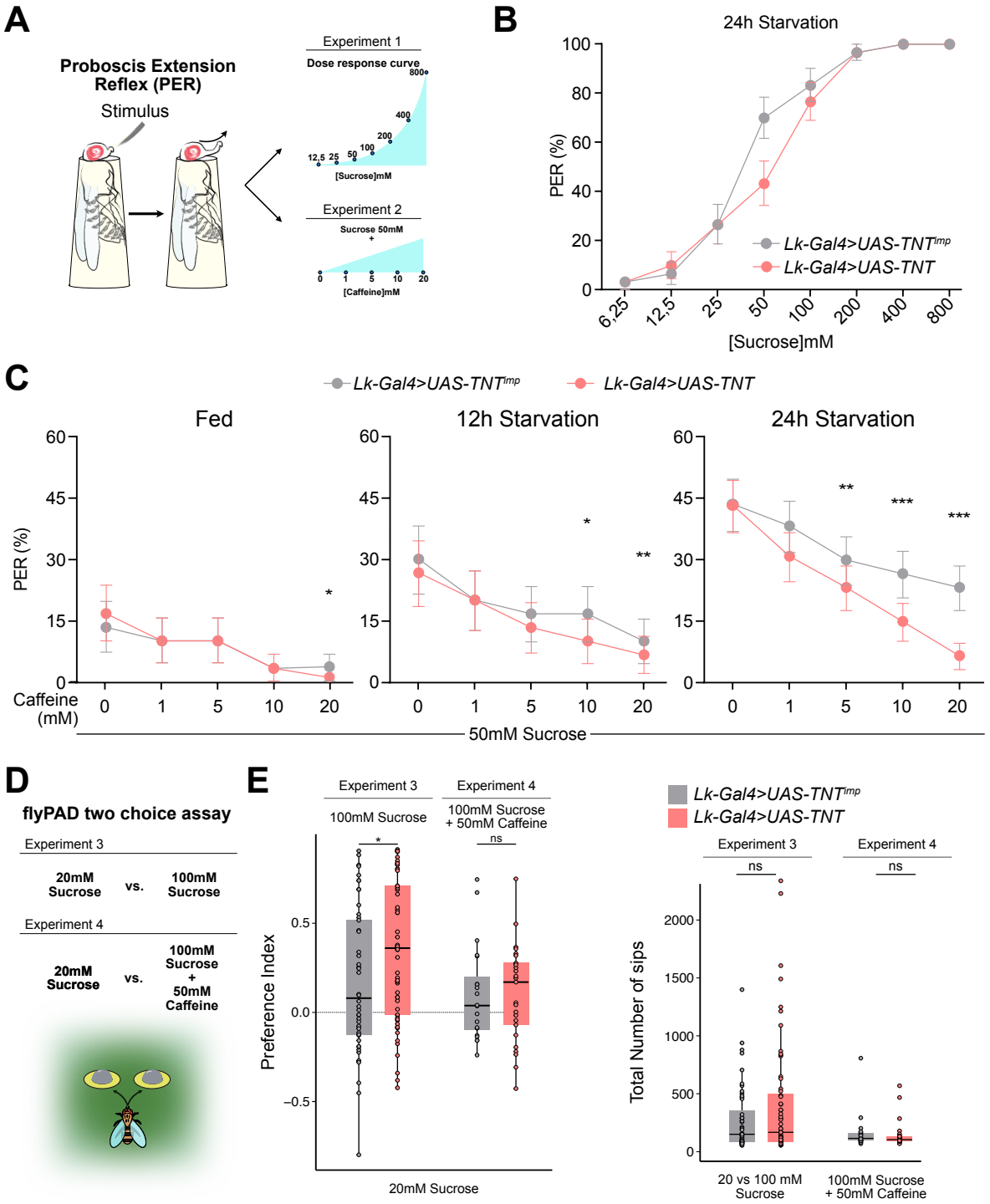

Figure 7. Leucokinin neurons integrate sweet and bitter gustatory information. (**A**) Scheme depicting the experimental procedure for Proboscis Extension Reflex (PER). Flies are given a series of increasing concentrations of sucrose (6.25, 12.5, 25, 50, 100, 200, 400 and 800 mM) for Experiment 1; and a fixed concentration of sucrose (50mM) mixed with increasing concentrations of caffeine (1, 5, 10 and 20mM) for Experiment 2. All flies starved 24 hours. (**B**) PER Dose response curve of *Lk-Gal4>UAS-TNT*^{imp} (n=30) and *Lk-Gal4>UAS-*

TNT (n=30) flies for Experiment 1. (**C**) PER of *Lk-Gal4>UAS-TNT*^{imp} (n=30) and *Lk-Gal4>UAS-TNT* (n=30) flies for Experiment 2. (**D**) Scheme depicting the experimental procedure for flyPAD (Adapted from Itskov et al., 2014). Experiment 3: 20mM Sucrose vs. 100mM Sucrose and Experiment 4: 20mM Sucrose vs. 100mM Sucrose + 50mM Caffeine. All flies starved 24 hours. (**E**) Preference Index (Left) for the highest concentration of Sucrose (100mM) with or without 50mM Caffeine and total number of sips (Right) for Experiment 3 and 4. Experiment 3: *Lk-Gal4>UAS-TNT*^{imp} (n=48); *Lk-Gal4>UAS-TNT* (n=59); Experiment 4: *Lk-Gal4>UAS-TNT*^{imp} (n=20); *Lk-Gal4>UAS-TNT* (n=25). Only flies that performed a minimum of 25 sips per fly and 2 bouts were considered for the analysis. ns: non-significant, *$p<0.05$. PER analysis: Binomial regression model; Error bars represent the standard error of the proportion. flyPAD statistics Wilcoxon Rank Sum Test.

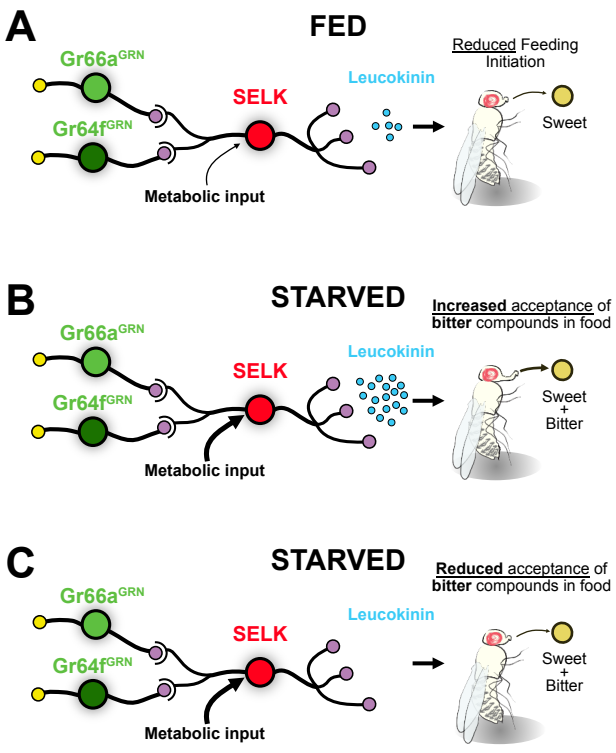

Figure 8. Model for the integration of gustatory information by SELK neurons. (**A**) SELK neurons receive direct input from Gr64f^{GRNs} (sweet), Gr66a^{GRNs} (bitter), and metabolic information. When flies are fed, the expression of the neuropeptide Leucokinin is reduced. The probability of a fed fly initiating feeding is reduced when facing any food. (**B**) SELK neurons in starved flies express large amounts of Leucokinin. In this situation, flies are more prone to accept food containing bitter compounds. (**C**) Starved flies with silenced SELK neurons are less prone to accept sweet foods laced with bitter compounds.

Materials and Methods

Key Resource Table

***Drosophila* strains**	**Source**		**Identifier**
Oregon-R	Kindly donated by Prof. Richard Benton		NA
w^{1118}	Kindly donated by Prof. Francisco Tejedor		NA
Gr64f-Gal4	Kindly donated by Prof. Richard Benton		NA
Gr64f-LexA	Kindly donated by Prof. Richard Benton		NA
Gr66a-Gal4	Bloomington Drosophila Stock Center		BDSC 57670
Gr66a-LexA; LexAop-rCD2:GFP	Kindly donated by Prof. Richard Benton		NA
LexAop-mCD8::GFP	Bloomington *Drosophila* Stock Center		BDSC 32203
Lk-Gal4	Bloomington *Drosophila* Stock Center		BDSC 51993
NompC-Gal4	Bloomington *Drosophila* Stock Center		BDSC 36361
NompC-LexA	Bloomington Drosophila Stock Center		BDSC 52240
QUAS-mtdTomato; retro-Tango; UAS-retro-Tango-GFP (*retro*-Tango)	Bloomington *Drosophila* Stock Center		BDSC 99661
UAS-DenMarK	Bloomington *Drosophila* Stock Center		BDSC 33062
UAS-mCD8:GFP	Bloomington *Drosophila* Stock Center		BDSC 32186
UAS-myrGFP, QUAS-mtdTomato; trans-Tango (*trans*-Tango)	Bloomington *Drosophila* Stock Center		BDSC 77124
UAS-TNT	Bloomington *Drosophila* Stock Center		BDSC 28837
UAS-TNT^{imp}	Bloomington *Drosophila* Stock Center		BDSC 28839
VGlut-Gal4	Bloomington *Drosophila* Stock Center		BDSC 24635
UAS-CD4-spGFP1-10, lexAop-CD4-spGFP11 (GRASP)	Bloomington *Drosophila* Stock Center		BDSC 58755
LexAop-GFP, LexAop-QF; UAS-B3RT, QUAS-mtdTomato (BAcTrace)	Bloomington *Drosophila* Stock Center		BDSC 90826
Primary antibodies	**Host species**	**Source**	**Working dilution**
Green Fluorescent Protein (GFP)	Chicken	Abcam (ab13970)	1:500
Red Fluorescent Protein (RFP)	Rabbit	Abcam (ab62341)	1:500
nc82 Bruchpilot	Mouse	DSHB	1:50
GFP reconstructed GRASP	Mouse	Sigma-Aldrich (G6539)	1:500
Leucokinin	Rat	Kindly donated by Prof. Pilar Herrero (de Haro et al., 2010)	1:100
Secondary Antibodies	**Host species**	**Source**	**Working dilution**
Green Fluorescent Protein (GFP)	Chicken	Abcam (ab13970)	1:500
Red Fluorescent Protein (RFP)	Rabbit	Abcam (ab62341)	1:500
nc82 Bruchpilot	Mouse	DSHB	1:50

Drosophila husbandry

Drosophila melanogaster stocks were reared and maintained on standard “Iberian” fly food under a 12 h light:12 h dark cycle at 25 ºC. *w*^{1118} and *Oregon-R* fly lines were used as mutant and wild-type strain controls unless otherwise indicated. Starvation was induced by transferring flies into vials containing a solid medium formed with a piece of paper (Kimberly-

Clark Kimtech, ref. 7552) soaked with 2,5 ml tap water. All *Drosophila* strains used in this thesis are listed in the Key Resource Table.

Tissue dissection and Fluorescence Activated Cell Sorting (FACS)

Central Brains or SEZs were dissected in cold Calcium- and Magnesium-free 1X Dulbecco's Phosphate Buffered Saline (DPBS) (ThermoFischer, ref. 14190094), transferred to a Protein LoBind (Eppendorf, ref. 0030108116) tube containing DPBS 0.01% BSA (Invitrogen, ref. AM2616) and digested with 1mg/ml of papain and collagenase (Sigma-Aldrich, ref. P4762 and C2674, respectively). After enzymatic digestion, dissociated tissue solution was filtered through a 20 µm filter (pluriSelect, ref. SKU 43-10020-40) into 300 µl DPBS BSA 0.01% in a Protein LoBind tube. Samples were kept at -80ºC or directly sorted by FACS.

Cells were sorted using a FACS AriaTM III. Several steps were followed to discard debris, clustered cells and dead cells using a DAPI fluorescent filter. Gustatory Second Order Neurons labeled with mtdTomato were selected using a 555 nm laser (RFP PE-Texas Red A) to discard non-fluorescent cells from the red fluorescent population. In addition to the 555 nm laser, to differentiate those autofluorescence (far red, λ > 670 nm) from actual mtdTomato *trans*-Tango signal from gustatory second-order neurons (λ = 615 nm), a far red 566 nm laser (PE-Cy7-A) was applied consecutively to only conserve those mtdTomato fluorescent single cells for PE-Texas Red-A laser and not for PE-Cy7-A laser (P6). All fluorescent gustatory second order neurons were sorted into Protein LowBind RNase-free tubes containing 15 µl of lysis buffer for RNA extraction and finally stored at -80ºC. To sort the Lk GFP^+ neurons from P4, the 488 nm laser was used to sort only GFP^+ fluorescent cells (P5) by applying the FITC-A filter.

Table 1. Number of brains and cells dissected

Fed Flies			Starved Flies		
Replicate	**#Brains dissected**	**#Cells collected**	**Replicate**	**#Brains dissected**	**#Cells collected**
Gr64f_1	406	21017	**Gr64f_1**	372	23126
Gr64f_2	512	23782	**Gr64f_2**	315	23387
Gr64f_3	191	21428	**Gr64f_3**	459	23267
Gr66a_1	519	21260	**Gr66a_1**	657	27555
Gr66a_2	531	21599	**Gr66a_2**	718	27090
Gr66a_3	594	21433	**Gr66a_3**	636	26991

RNAseq analysis

RNA extraction and sequencing

RNA was extracted using the PicoArcturus RNA isolation kit (ThermoFisher, ref. 12204-01). The spectrophotometer NanoDrop® ND-1000 was used for samples estimated to contain higher amounts of total mRNA extracted, in the range of 100-3.000 ng/µl. Additionally, to obtain the exact concentration and test the mRNA's quality, total mRNA was measured using the 2100 Bioanalyzer (Agilent Technologies). 50 to 5.000 pg/µl range was measured using chips from the RNA 6.000 Pico Kit (Agilent Technologies).

Samples were sequenced using 50 bp single reads on an *Illumina HiSeq2500* (for fed condition) and *Illumina NextSEq2000* (for starved condition) sequencers at the Genomics Unit of the Center for Genomic Regulation (Barcelona, Spain).

Reads were quality-checked with MultiQC v1.0 software using the tool FastQC v0.11.9. RNAseq output reads were aligned to the *D. melanogaster* reference genome from the Ensemble Project database (EMBL-EBI, Cambridge, UK) using STAR v2.7.9a (Spliced Transcripts Alignment to a Reference)[68]. Differential gene expression analysis was performed using DESeq2 v1.28.1[69] with the free *R* programming language (GNU project) software *RStudio* v4.2. Also, the reads within the gene were transformed by this tool to a total of counts per gene. Transcripts per million (TPM) were calculated using Salmon 1.10.2[70]. A combination of packages (or libraries) from CRAN and Bioconductor v3.14[71,72] open-source projects were used for data processing and plotting.

Gene Ontology analysis

The Gene Ontology (GO) analysis was performed using the open source interface PANGEA (Pathway, Network and Gene-set Enrichment Analysis; https://www.flyrnai.org/tools/pangea/)[73] specifically the *Drosophila* GO subsets terms at the online platform. Only those genes significantly up-regulated or significantly down-regulated in the differential gene expression analysis were included in the GO analysis. Each of the G2N's differential expressed genes was analyzed separately, and then, only those GO terms of interest were plotted in one single graph.

Additionally, other GO analysis interfaces and tools as g::Profiler (https://biit.cs.ut.ee/gprofiler/gost), AmiGO2 (https://amigo.geneontology.org/amigo) undefined were used to validate the results of PANGEA. Finally, Gene set enrichment analysis (GSEA) was represented using RStudio v4.2 software (code available upon request).

qPCR

Standard real-time quantitative PCR (qPCR) was performed with 2 ng of template cDNA, PowerUp SYBR Green PCR Master Mix (Applied Biosystems, ref. A25742) and gene-specific primers read on QuantStudio 3 Real-Time PCR System (Applied Biosystems, ref. A28567) with a standard cycling mode: 2 min at 50ºC and another 2 minutes at 95ºC followed by 40x cycles of 15 seconds at 95ºC and 1 min at 60ºC. *Gapdh2* (Glyceraldehyde 3 phosphate dehydrogenase 2) of *D. melanogaster* protein expression levels was used as a housekeeping gene to normalize the results. Triplicate samples per each condition and technical triplicates were performed, and the relative gene expression was normalized by ΔCt analysis. Data is presented as mean ± SEM, and was statistically analyzed using two-tailed Student's *t*-test, considering *p*-value < 0,05 to be statistically significant. Primers used:

Gene	Forward sequence (5' to 3')	Reverse sequence (5' to 3')
LK[39]	GCCTTTGGCCGTCAAGTCTA	TGAACCTGCGGTACTTGGAG
Gapdh2[75]	CTACCTGTTCAAGTTCGATTCGAC	AGTGGACTCCACGATGTATTC

Immunohistochemistry

Immunofluorescence on peripheral and central tissues of adult flies was performed following standard procedures [76,77]. In brief, brains and proboscis were dissected in cold phosphate buffer (PB) and fixed for 25 minutes in 4% paraformaldehyde (PFA EMS15710) in PB at RT. After that, brains and proboscis were washed 5 times for 10 minutes with PB + 0.3% Triton X-100 (PBT) and blocked for 1 hour in PBT + 5% normal goad serum (NGS) (Abcam, ref. ab7481). Later, primary and secondary antibody (See Key Resource Table) incubations were for 48h each in PBT + 5% NGS at 4ºC in constant agitation. Finally, after 5 washes of 10 minutes, brains and proboscis were equilibrated and mounted in Vectashield Antifade Mounting Medium with DAPI (Vector Laboratories, ref. H-1200-10), maintaining their three-dimensional structure.

Microscopy image capture and processing

Images were acquired using a Leica SPEII laser scanning confocal microscope. Routinely, images of dimensions 512x512 pixels were acquired using an oil immersion 20x objective in stacks of 1-2 µm. Files were saved in *.tiff* format and processed with ImageJ (Fiji) open-source image-processing software[78]. For fluorescence quantification, the fluorescent intensity from the Region Of Interest (ROI) area was analyzed by using the ROI Manager from ImageJ, and data is presented as mean ± standard error of the mean (SEM) and was statistically analyzed using two-tailed Student's *t*-test, considering *p*-value < 0,05 to be statistically significant.

Electron microscopy neural reconstructions and connectivity

Candidate neurons were reconstructed in a serial section transmission electron volume [49] using FlyWire (https://flywire.ai/) [52,79]. To do that, from the open-source interface of Virtual Fly Brain (VFB)[80], several sweet and bitter GRNs skeletons (.*swc* format) described previously were downloaded[50]. A total of 52 GRN skeletons were downloaded from the VFB dataset in .swc format and aligned to the FAFB by using the JRC2018U reference brain as a template [49,81,82]. From these, 19 GRNs were bitter sensing (12 from group 1 (**Suplementary Figure 6A-A'**) and 7 from group 2 (**Sup Figure 6B-B'**)), and 33 GRNs were sweet sensing (17 from group 4 (**Suplementary Figure 6C-C'**) and 16 from group 5 (**Suplementary Figure 6D-D'**)). Only $Gr64f^{GRN}$ and $Gr66a^{GRN}$ of the right hemisphere were used in this analysis as the dataset is larger. All these GRN skeletons were aligned to the recently released FlyWire dataset, a dense, machine learning-based reconstruction of more than 80,000 FAFB neurons [51,79] (for more detail, see materials and methods). By using the Flywire Gateway tool, each of the sweet and bitter GRNs analyzed was aligned and reconstructed to the EM dataset (**Suplementary Figure 6E-F''**) in the FlyWire toolbox, where a brain mesh template was used to represent the morphology of the tracing aligned (**Suplementary Figure 6G-L**) and the IDs annotated[79]. All skeletons were aligned to FlyWire dataset[79] by using the Flywire Gateway tool, taking as a reference the JRC2018U reference brain[81]. All Flywire IDs for the sweet and bitter GRNs analyzed were identified from this skeleton alignment.

To identify synaptic partners to the Flywire IDs identified, the open-source BrainCircuits[53] interface (https://braincircuits.io/app?p=fruitfly_fafb_flywire_public) was used by uploading the FlyWire IDs in the "Connectivity" tool space. Briefly, BrainCircuits is an interface based on AI and human neural reconstractions to map out the neuronal connections within the *Drosophila* brain. Those IDs with synaptic points with sweet and bitter GRNs were selected as candidates. Then, according to previous morphological immunohistochemistry experiments, manual and visual criteria were applied to identify the neurons of interest. The Flywire Codex platform was used to find morphological similar neurons to those identified[83]. On the other hand, for other applications, only upstream and downstream IDs with ≥10 synaptic sites were selected as presynaptic and postsynaptic candidates.

Final FAFB reconstructions were done using FlyWire Sandbox and virtual reconstructed neuron images were taken by online screenshots.

Behavior

Proboscis Extension Reflex(PER)

PER to labellar stimulation was assessed following a standard protocol[84]. Flies were anesthetized on ice and individually immobilized on P200 tips, whose narrow end was cut so that only the fly's head could protrude from the opening, leaving the rest of the body, including

legs, constrained inside the tip. After flies were recovered in a humidified chamber for 20 min, flies were water-satiated before testing *ad libitum*, discarding those that, after 5 min, continued extending their proboscis in response to water. Tastants were delivered using a small piece of paper (Kimberly-Clark Kimtech, ref. 7552) and touching very gently the labellum for 2 s maximum, leaving a gap of 1 min between stimulations. Sucrose (Sigma Aldrich, ref. 102174662) and Caffeine (Sigma-Aldrich, ref. 102143502) were diluted in miliQ sterile water appropriately. PER was manually recorded: only full proboscis extensions were counted as PER and registered as 1, considering partial or absent proboscis extension as 0. Finally, flies were tested at the end of the experiment with water as the negative control and 1 M of sucrose as the positive control. Only flies that showed negative PER for water and positive PER for 1 M of sucrose were included in the analysis.

flyPAD two choice assay

flyPAD assays were performed to study the feeding microstructure in a two-choice feeding paradigm as described previously[57], and several feeding parameters were measured individually in a high throughput manner. Individual flies were placed in individual arenas with two different food sources in independent well electrodes. The flyPAD hardware used comprised 56 individual chambers divided into two independent pieces of hardware, each consisting of 28 chambers connected to an independent computer.All tastants used were solved in water 1% low melt agarose (Lonza, ref. 50100). To transfer files to each chamber, flies were anesthetized in ice for 5 min and individually placed in the arena by mouth aspiration according to its sex and genotype. All the experiments began once all flies woke up and were active. Flies were allowed to feed at 25ºC for 60 min. After time ended, dead flies were annotated.flyPAD data were acquired using the Bonsai framework, and analyzed in MATLAB using custom-written software delivered by *Itskov et al., 2014*[57],. Then, specific *R* software scripts developed by the lab were applied to analyze the bulk of flyPAD experiment data. Only those flies that performed more than 2 bouts and 25 sips were included in the analysis.

Statistical analysis

The sample size was determined based on preliminary experiments. Data were analyzed using *R* software v4.1.0 (R Foundation for Statistical Computing, Vienna, Austria, 2005; https://www.r-project.org) (code available upon request) and plotted using *R* or *Graphpad Prisms 6*. The statistical test is determined in the figure legend for each of the plots. The Bonferroni method was used when p-value correction for multiple comparisons was required. Except for PER and flyPAD experiments, quantitative data show their distribution by superimposing a boxplot. For the boxplots the whiskers are calculated as follows: the upper whisker equals the third quartile plus 1.5× the interquartile range (IQR) and the lower whisker

equals the first quartile minus 1.5× the IQR. Any data points above the superior or below the inferior whisker values are considered outliers. The outliers were included in the statistical comparisons as we performed non-parametric rank tests.

For PER experiments, data were analyzed using a logistic regression set to a binomial distribution model (function lm () in R software), and error bars represent the standard error of the proportion ($\sqrt{p(1-p)/n}$). For flyPAD experiments, a set of *R* software scrips developed by the lab was used to analyze the feeding microstructure behavior, which employs different statistical tests depending on the final goal of the analysis. The preference index is calculated as follows:

$$\text{Preference Index (PI)} = \frac{N_A - N_B}{N_{TOTAL}}$$

Bibliography

1. Chu, B., Chui, V., Mann, K. & Gordon, M. D. Presynaptic Gain Control Drives Sweet and Bitter Taste Integration in Drosophila. *Curr Biol* **24**, 1978–1984 (2014).

2. Inagaki, H. K., Panse, K. M. & Anderson, D. J. Independent, Reciprocal Neuromodulatory Control of Sweet and Bitter Taste Sensitivity during Starvation in Drosophila. *Neuron* **84**, 806–820 (2014).

3. LeDue, E. E. *et al.* Starvation-Induced Depotentiation of Bitter Taste in Drosophila. *Curr Biol* **26**, 2854–2861 (2016).

4. Yarmolinsky, D. A. *et al.* Coding and Plasticity in the Mammalian Thermosensory System. *Neuron* **92**, 1079–1092 (2016).

5. Vosshall, L. B. & Stocker, R. F. Molecular Architecture of Smell and Taste in Drosophila. *Annu Rev Neurosci* **30**, 505–533 (2007).

6. Montell, C. Drosophila sensory receptors—a set of molecular Swiss Army Knives. *Genetics* **217**, 1–34 (2021).

7. Dahanukar, A., Lei, Y.-T., Kwon, J. Y. & Carlson, J. R. Two Gr Genes Underlie Sugar Reception in Drosophila. *Neuron* **56**, 503–516 (2007).

8. Fujii, S. *et al.* Drosophila Sugar Receptors in Sweet Taste Perception, Olfaction, and Internal Nutrient Sensing. *Curr Biol* **25**, 621–627 (2015).

9. Dunipace, L., Meister, S., McNealy, C. & Amrein, H. Spatially restricted expression of candidate taste receptors in the Drosophila gustatory system. *Curr. Biol.* **11**, 822–835 (2001).

10. Wang, Z., Singhvi, A., Kong, P. & Scott, K. Taste Representations in the Drosophila Brain. *Cell* **117**, 981–991 (2004).

11. Scott, K. Gustatory Processing in Drosophila melanogaster. *Annu Rev Entomol* **63**, 15–30 (2018).

12. Jenett, A. *et al.* A GAL4-Driver Line Resource for Drosophila Neurobiology. *Cell Reports* **2**, 991–1001 (2012).
13. Dionne, H., Hibbard, K. L., Cavallaro, A., Kao, J.-C. & Rubin, G. M. Genetic Reagents for Making Split-GAL4 Lines in Drosophila. *Genetics* **209**, 31–35 (2018).
14. Meissner, G. W. *et al.* A searchable image resource of Drosophila GAL4 driver expression patterns with single neuron resolution. *eLife* **12**, e80660 (2023).
15. Flood, T. F. *et al.* A single pair of interneurons commands the Drosophila feeding motor program. *Nature* **499**, 83–87 (2013).
16. Kain, P. & Dahanukar, A. Secondary Taste Neurons that Convey Sweet Taste and Starvation in the Drosophila Brain. *Neuron* **85**, 819–832 (2015).
17. Miyazaki, T., Lin, T.-Y., Ito, K., Lee, C.-H. & Stopfer, M. A gustatory second-order neuron that connects sucrose-sensitive primary neurons and a distinct region of the gnathal ganglion in the Drosophila brain. *J. Neurogenet.* **29**, 144–155 (2015).
18. Yapici, N., Cohn, R., Schusterreiter, C., Ruta, V. & Vosshall, L. B. A Taste Circuit that Regulates Ingestion by Integrating Food and Hunger Signals. *Cell* **165**, 715–729 (2016).
19. Kim, H., Kirkhart, C. & Scott, K. Long-range projection neurons in the taste circuit of Drosophila. *eLife* **6**, e23386 (2017).
20. Schwarz, O. *et al.* Motor control of Drosophila feeding behavior. *Elife* **6**, e19892 (2017).
21. Bohra, A. A., Kallman, B. R., Reichert, H. & VijayRaghavan, K. Identification of a Single Pair of Interneurons for Bitter Taste Processing in the Drosophila Brain. *Curr. Biol.* **28**, 847-858.e3 (2018).
22. The Olfactory System, From Odor Molecules to Motivational Behaviors. (2014) doi:10.1007/978-4-431-54376-3.
23. Sterne, G. R., Otsuna, H., Dickson, B. J. & Scott, K. Classification and genetic targeting of cell types in the primary taste and premotor center of the adult Drosophila brain. *Elife* **10**, e71679 (2021).
24. Talay, M. *et al.* Transsynaptic Mapping of Second-Order Taste Neurons in Flies by trans-Tango. *Neuron* **96**, 783-795.e4 (2017).
25. Weiss, L. A., Dahanukar, A., Kwon, J. Y., Banerjee, D. & Carlson, J. R. The Molecular and Cellular Basis of Bitter Taste in Drosophila. *Neuron* **69**, 258–272 (2011).
26. Root, C. M., Ko, K. I., Jafari, A. & Wang, J. W. Presynaptic Facilitation by Neuropeptide Signaling Mediates Odor-Driven Food Search. *Cell* **145**, 133–144 (2011).
27. Krashes, M. J. *et al.* A Neural Circuit Mechanism Integrating Motivational State with Memory Expression in Drosophila. *Cell* **139**, 416–427 (2009).
28. Riemensperger, T. *et al.* Behavioral consequences of dopamine deficiency in the Drosophila central nervous system. *Proc. Natl. Acad. Sci.* **108**, 834–839 (2011).

29. Nässel, D. R. & Zandawala, M. Recent advances in neuropeptide signaling in Drosophila, from genes to physiology and behavior. *Prog Neurobiol* **179**, 101607 (2019).
30. Farhan, A. *et al.* The CCHamide 1 receptor modulates sensory perception and olfactory behavior in starved Drosophila. *Sci Rep-uk* **3**, 2765 (2013).
31. Inagaki, H. K. *et al.* Visualizing Neuromodulation In Vivo: TANGO-Mapping of Dopamine Signaling Reveals Appetite Control of Sugar Sensing. *Cell* **148**, 583–595 (2012).
32. Jaeger, A. H. *et al.* A complex peripheral code for salt taste in Drosophila. *Elife* **7**, e37167 (2018).
33. Lee, K.-S., You, K.-H., Choo, J.-K., Han, Y.-M. & Yu, K. Drosophila Short Neuropeptide F Regulates Food Intake and Body Size*. *J. Biol. Chem.* **279**, 50781–50789 (2004).
34. Wu, Q. *et al.* Developmental Control of Foraging and Social Behavior by the Drosophila Neuropeptide Y-like System. *Neuron* **39**, 147–161 (2003).
35. Yoshinari, Y. *et al.* The sugar-responsive enteroendocrine neuropeptide F regulates lipid metabolism through glucagon-like and insulin-like hormones in Drosophila melanogaster. *Nat. Commun.* **12**, 4818 (2021).
36. Cannell, E. *et al.* The corticotropin-releasing factor-like diuretic hormone 44 (DH44) and kinin neuropeptides modulate desiccation and starvation tolerance in Drosophila melanogaster. *Peptides* **80**, 96–107 (2016).
37. Nässel, D. R. Leucokinin and Associated Neuropeptides Regulate Multiple Aspects of Physiology and Behavior in Drosophila. *Int J Mol Sci* **22**, 1940 (2021).
38. Haro, M. de *et al.* Detailed analysis of leucokinin-expressing neurons and their candidate functions in the Drosophila nervous system. *Cell Tissue Res.* **339**, 321–336 (2010).
39. Zandawala, M. *et al.* Modulation of Drosophila post-feeding physiology and behavior by the neuropeptide leucokinin. *Plos Genet* **14**, e1007767 (2018).
40. Al-Anzi, B. *et al.* The Leucokinin Pathway and Its Neurons Regulate Meal Size in Drosophila. *Curr Biol* **20**, 969–978 (2010).
41. Murakami, K. *et al.* translin Is Required for Metabolic Regulation of Sleep. *Curr. Biol.* **26**, 972–980 (2016).
42. Murphy, K. R. *et al.* Postprandial sleep mechanics in Drosophila. *Elife* **5**, e19334 (2016).
43. Yurgel, M. E. *et al.* A single pair of leucokinin neurons are modulated by feeding state and regulate sleep–metabolism interactions. *Plos Biol* **17**, e2006409 (2019).
44. Raji, J. I. & Potter, C. J. The number of neurons in Drosophila and mosquito brains. *Plos One* **16**, e0250381 (2021).
45. Asahina, K. *et al.* Tachykinin-Expressing Neurons Control Male-Specific Aggressive Arousal in Drosophila. *Cell* **156**, 221–235 (2014).
46. Feinberg, E. H. *et al.* GFP Reconstitution Across Synaptic Partners (GRASP) Defines Cell Contacts and Synapses in Living Nervous Systems. *Neuron* **57**, 353–363 (2008).

47. Thistle, R., Cameron, P., Ghorayshi, A., Dennison, L. & Scott, K. Contact Chemoreceptors Mediate Male-Male Repulsion and Male-Female Attraction during Drosophila Courtship. *Cell* **149**, 1140–1151 (2012).
48. Cachero, S. *et al.* BAcTrace, a tool for retrograde tracing of neuronal circuits in Drosophila. *Nat Methods* **17**, 1254–1261 (2020).
49. Zheng, Z. *et al.* A Complete Electron Microscopy Volume of the Brain of Adult Drosophila melanogaster. *Cell* **174**, 730-743.e22 (2018).
50. Engert, S., Sterne, G. R., Bock, D. D. & Scott, K. Drosophila gustatory projections are segregated by taste modality and connectivity. *Elife* **11**, e78110 (2022).
51. Eckstein, N. *et al.* Neurotransmitter Classification from Electron Microscopy Images at Synaptic Sites in Drosophila Melanogaster. *bioRxiv* 2020.06.12.148775 (2023) doi:10.1101/2020.06.12.148775.
52. Schlegel, P. *et al.* Whole-brain annotation and multi-connectome cell typing quantifies circuit stereotypy in Drosophila. *bioRxiv* 2023.06.27.546055 (2023) doi:10.1101/2023.06.27.546055.
53. Gerhard, S., Lee, W.-C. A. & Wilson, R. The BrainCircuits.io platform. https://braincircuits.io/. (2023).
54. Sorkaç, A. *et al.* retro-Tango enables versatile retrograde circuit tracing in Drosophila. *eLife* **12**, e85041 (2023).
55. Sweeney, S. T., Broadie, K., Keane, J., Niemann, H. & O'Kane, C. J. Targeted expression of tetanus toxin light chain in Drosophila specifically eliminates synaptic transmission and causes behavioral defects. *Neuron* **14**, 341–351 (1995).
56. French, A. S. *et al.* Dual Mechanism for Bitter Avoidance in Drosophila. *J Neurosci* **35**, 3990–4004 (2015).
57. Itskov, P. M. *et al.* Automated monitoring and quantitative analysis of feeding behaviour in Drosophila. *Nat Commun* **5**, 4560 (2014).
58. Snell, N. J. *et al.* Complex representation of taste quality by second-order gustatory neurons in Drosophila. *Curr Biol* **32**, 3758-3772.e4 (2022).
59. Kiral, F. R. *et al.* Brain connectivity inversely scales with developmental temperature in Drosophila. *Cell Reports* **37**, 110145 (2021).
60. Scaplen, K. M. *et al.* Transsynaptic mapping of Drosophila mushroom body output neurons. *Elife* **10**, e63379 (2021).
61. Ehrlich, A. *et al.* Tango-seq: overlaying transcriptomics on connectomics to identify neurons downstream of Drosophila clock neurons. *bioRxiv* 2024.05.22.595372 (2024) doi:10.1101/2024.05.22.595372.
62. Yarmolinsky, D. A., Zuker, C. S. & Ryba, N. J. P. Common Sense about Taste: From Mammals to Insects. *Cell* **139**, 234–244 (2009).

63. Barretto, R. P. J. *et al.* The neural representation of taste quality at the periphery. *Nature* **517**, 373–376 (2015).

64. Chen, X., Gabitto, M., Peng, Y., Ryba, N. J. P. & Zuker, C. S. A Gustotopic Map of Taste Qualities in the Mammalian Brain. *Science* **333**, 1262–1266 (2011).

65. Wang, L. *et al.* The coding of valence and identity in the mammalian taste system. *Nature* **558**, 127–131 (2018).

66. Harris, D. T., Kallman, B. R., Mullaney, B. C. & Scott, K. Representations of Taste Modality in the Drosophila Brain. *Neuron* **86**, 1449–1460 (2015).

67. Gordon, M. D. & Scott, K. Motor Control in a Drosophila Taste Circuit. *Neuron* **61**, 373–384 (2009).

68. Dobin, A. *et al.* STAR: ultrafast universal RNA-seq aligner. *Bioinformatics* **29**, 15–21 (2012).

69. Love, M. I., Huber, W. & Anders, S. Moderated estimation of fold change and dispersion for RNA-seq data with DESeq2. *Genome Biol.* **15**, 550 (2014).

70. Roberts, A., Trapnell, C., Donaghey, J., Rinn, J. L. & Pachter, L. Improving RNA-Seq expression estimates by correcting for fragment bias. *Genome Biol.* **12**, R22 (2011).

71. Gentleman, R. C. *et al.* Bioconductor: open software development for computational biology and bioinformatics. *Genome Biol.* **5**, R80 (2004).

72. Huber, W. *et al.* Orchestrating high-throughput genomic analysis with Bioconductor. *Nat. Methods* **12**, 115–121 (2015).

73. Hu, Y. *et al.* PANGEA: a new gene set enrichment tool for Drosophila and common research organisms. *Nucleic Acids Res.* **51**, W419–W426 (2023).

74. Ashburner, M. *et al.* Gene Ontology: tool for the unification of biology. *Nat. Genet.* **25**, 25–29 (2000).

75. Uchizono, S. *et al.* Deciphering the Genes for Taste Receptors for Fructose in Drosophila. *Mol Cells* **40**, 731–736 (2017).

76. Croset, V. *et al.* Ancient Protostome Origin of Chemosensory Ionotropic Glutamate Receptors and the Evolution of Insect Taste and Olfaction. *Plos Genet* **6**, e1001064 (2010).

77. Sánchez-Alcañiz, J. A., Zappia, G., Marion-Poll, F. & Benton, R. A mechanosensory receptor required for food texture detection in Drosophila. *Nat Commun* **8**, 14192 (2017).

78. Schindelin, J. *et al.* Fiji: an open-source platform for biological-image analysis. *Nat. Methods* **9**, 676–682 (2012).

79. Dorkenwald, S. *et al.* FlyWire: online community for whole-brain connectomics. *Nat Methods* **19**, 119–128 (2022).

80. Milyaev, N. *et al.* The Virtual Fly Brain browser and query interface. *Bioinformatics* **28**, 411–415 (2011).

81. Bogovic, J. A. *et al.* An unbiased template of the Drosophila brain and ventral nerve cord. *PLoS ONE* **15**, e0236495 (2020).

82. Costa, M., Manton, J. D., Ostrovsky, A. D., Prohaska, S. & Jefferis, G. S. X. E. NBLAST: Rapid, Sensitive Comparison of Neuronal Structure and Construction of Neuron Family Databases. *Neuron* **91**, 293–311 (2016).

83. Matsliah, A. *et al.* Codex: Connectome Data Explorer. *bioRxiv* (2023) doi:10.13140/rg.2.2.35928.67844.

84. Shiraiwa, T. & Carlson, J. R. Proboscis Extension Response (PER) Assay in Drosophila. *J Vis Exp* 193 (2007) doi:10.3791/193.